ACTA MECHANICA SINICA (English Series), Vol.15, No.4, Nov. 1999 ISSN 0567-7718
The Chinese Society of Theoretical and Applied Mechanics
Chinese Journal of Mechanics Press, Beijing, China
Allerton Press, INC., New York, U.S.A.

SOME WEIGHT-TYPE HIGH-RESOLUTION DIFFERENCE SCHEMES AND THEIR APPLICATIONS*

Wang Ruquan (王汝权)
(*Institute of Computational Mathematics and Scientific/Engineering Computing, Chinese Academy of Sciences, Beijing* 100080, *China*)

Shen Yiqing (申义庆)
(*LHD, Institute of Mechanics, Chinese Academy of Sciences, Beijing* 100080, *China*)

ABSTRACT: By the aid of an idea of the weighted ENO schemes, some weight-type high-resolution difference schemes with different orders of accuracy are presented in this paper by using suitable weights instead of the minmod functions appearing in various TVD schemes. Numerical comparisons between the weighted schemes and the non-weighted schemes have been done for scalar equation, one-dimensional Euler equations, two-dimensional Navier-Stokes equations and parabolized Navier-Stokes equations.

KEY WORDS: TVD schemes, ENO schemes, WENO schemes, Euler equations, Navier-Stokes equations

1 INTRODUCTION

At present the high-resolution TVD schemes have been widely applied to solve the Euler equations and Navier-Stokes equations. However, many numerical experiments showed that the second-order accurate TVD schemes can not simulate accurately separated vortices and complicated viscous flow fields. This is due to the fact that the second-order TVD schemes degenerate to the first-order at extrema. Although the ENO schemes may achieve any high-order accuracy, they are not convenient in practice. In 1994, Liu, Osher and Chan[1] first introduced the concept of the weighted ENO schemes and constructed an $(r+1)$th order weighted ENO schemes based on the rth order ENO schemes with the same stencils. Recently, Jiang and Shu[2] presented an efficient implementation of the weighted ENO schemes based on flux version instead of cell-averaged version.

If the minmod functions used in the various TVD schemes are replaced by suitable weights, would the accuracy order of the TVD-type difference schemes be improved or not? The answer is affirmative. To describe in detail the above mentioned idea, we choose the second-order NND scheme[3] and third-order ENN scheme[4] in flux version as the non-weighted basic schemes.

Received 5 June 1998, revised 17 June 1999
* The project supported by the National Natural Science Foundation of China (19582007) and Partly by State Key Laboratory of Scientific/Engineering Computing.

In this paper we will construct a weight-type non-oscillatory dissipation (WND) scheme and two weight-type essentially non-oscillatory (WEN) schemes based on the NND and ENN schemes, respectively. The weighted WND and WEN schemes have the same orders as the NND and ENN schemes and improve significantly the accuracy of the NND and ENN schemes near the extrema and in the vortex regions of viscous flows and the rate of convergence to steady solution. These features are very interesting for solving multi-dimensional viscous flow problems with vortices.

2 DIFFERENCE SCHEMES FOR SCALAR EQUATION

Consider a scalar conservative hyperbolic equation

$$\frac{\partial u}{\partial t} + \frac{\partial f(u)}{\partial x} = 0 \tag{2.1}$$

where $f(u)$ is a flux function and may be splitted into two parts $f(u) = f^+(u) + f^-(u)$, $\frac{\mathrm{d}f^+(u)}{\mathrm{d}u} \geq 0$, $\frac{\mathrm{d}f^-(u)}{\mathrm{d}u} < 0$. In this paper we define $f^{\pm}(u) = \frac{1}{2}(f(u) \pm \alpha u)$ and $\alpha = \max|f'(u)|$. The semi-discrete conservative difference scheme can be written as follows

$$\frac{\mathrm{d}v_j}{\mathrm{d}t} + \frac{(h_{j+1/2} - h_{j-1/2})}{\Delta x} = 0 \tag{2.2}$$

where $v = \frac{1}{\Delta x}\int_{x_{j-1/2}}^{x_{j+1/2}} u\mathrm{d}x$ and the numerical flux $h_{j+1/2} = h^+_{j+1/2} + h^-_{j-1/2}$ may have different forms for different methods. In the following, we will rewrite the original NND and ENN schemes, proposed by Zhang et al. in [3] and [4], separately, and then construct the weight-type schemes.

2.1 Second-Order WND Scheme

The second-order NND scheme of Eq.(2.1) has the following numerical fluxes

$$\left.\begin{aligned} h^+_{j+1/2} &= f^+_j + \frac{1}{2}\mathrm{ms}(\Delta f^+_{j+1/2}, \Delta f^+_{j-1/2}) \\ h^-_{j+1/2} &= f^-_{j+1} - \frac{1}{2}\mathrm{ms}(\Delta f^-_{j+3/2}, \Delta f^-_{j+1/2}) \end{aligned}\right\} \tag{2.3}$$

where the limiter $\mathrm{ms}(a, b)$ is defined as follows

$$\mathrm{ms}(a,b) = \begin{cases} a & |a| \leq |b| \\ b & |a| > |b| \end{cases} \tag{2.4}$$

It is clear that the scheme(2.3) may achieve second-order accuracy, if $\mathrm{ms}(\Delta f^+_{j+1/2}, \Delta f^+_{j-1/2})$ and $\mathrm{ms}(\Delta f^-_{j+3/2}, \Delta f^-_{j+1/2})$ will be replaced by $\frac{1}{2}(\Delta f^+_{j+1/2} + \Delta f^+_{j-1/2})$ and $\frac{1}{2}(\Delta f^-_{j+3/2} + \Delta f^-_{j+1/2})$, respectively.

Unfortunately, the second-order scheme will produce oscillatory numerical solutions near the discontinuities. To overcome this drawback, we can use proper weighted functions ω_j instead of the arithmetic average. The form of the weighted functions is similar to that

in the WENO schemes[1,2]. We present numerical fluxes of the WND scheme as follows

$$\left.\begin{aligned} h^+_{j+1/2} &= f^+_j + \frac{1}{2}(\omega^+_0 \Delta f^+_{j+1/2} + \omega^+_1 \Delta f^+_{j-1/2}) \\ h^-_{j+1/2} &= f^-_{j+1} - \frac{1}{2}(\omega^-_0 \Delta f^-_{j+3/2} + \omega^-_1 \Delta f^-_{j+1/2}) \end{aligned}\right\} \tag{2.5}$$

where

$$\omega^+_0 = \frac{\alpha^+_0}{\alpha^+_0 + \alpha^+_1} \qquad \omega^+_1 = \frac{\alpha^+_1}{\alpha^+_0 + \alpha^+_1} \qquad \omega^-_0 = \frac{\alpha^-_0}{\alpha^-_0 + \alpha^-_1}$$

$$\omega^-_1 = \frac{\alpha^-_1}{\alpha^-_0 + \alpha^-_1} \qquad \alpha^+_0 = \frac{1}{\varepsilon + (|\Delta f^+_{j+1/2}|)^p} \qquad \alpha^+_1 = \frac{1}{\varepsilon + (|\Delta f^+_{j-1/2}|)^p}$$

$$\alpha^-_0 = \frac{1}{\varepsilon + (|\Delta f^-_{j+3/2}|)^p} \qquad \alpha^-_1 = \frac{1}{\varepsilon + (|\Delta f^-_{j+1/2}|)^p}$$

where $\varepsilon = 10^{-10}$ and $p \geq 1.0$ ($p = 1.0$ in this paper).

Clearly, the WND scheme(2.5) keeps the same order of accuracy in the smooth regions and the non-oscillatory property near the discontinuities, but it will approach the second-order central scheme at the extrema and in the smooth plateau regions of solution.

2.2 Third-Order WEN Schemes

In 1993, Zhang et al.[4] developed a third-order accurate ENN scheme of Eq.(2.1), which has numerical fluxes as follows

$$h^+_{j+1/2} = \begin{cases} f^+_j + \frac{1}{2}\Delta f^+_{j+1/2} - \frac{1}{6}\mathrm{ms}(D^+_j, D^+_{j+1}) & \text{if} \quad |\Delta f^+_{j+1/2}| \leq |\Delta f^+_{j-1/2}| \\ f^+_j + \frac{1}{2}\Delta f^+_{j-1/2} + \frac{1}{3}\mathrm{ms}(D^+_j, D^+_{j-1}) & \text{if} \quad |\Delta f^+_{j+1/2}| > |\Delta f^+_{j-1/2}| \end{cases} \tag{2.6}$$

$$h^-_{j+1/2} = \begin{cases} f^-_{j+1} - \frac{1}{2}\Delta f^-_{j+3/2} + \frac{1}{3}\mathrm{ms}(D^-_{j+1}, D^-_{j+2}) & \text{if} \quad |\Delta f^-_{j+3/2}| \leq |\Delta f^-_{j+1/2}| \\ f^-_{j+1} - \frac{1}{2}\Delta f^-_{j+1/2} - \frac{1}{6}\mathrm{ms}(D^-_j, D^-_{j+1}) & \text{if} \quad |\Delta f^-_{j+3/2}| > |\Delta f^-_{j+1/2}| \end{cases} \tag{2.7}$$

where $D_j = \Delta f_{j+1/2} - \Delta f_{j-1/2}$. Following the above mentioned WND scheme, we can also construct corresponding weight-type schemes from the ENN scheme which keep the same accuracy and non-oscillatory property. The ENN and WEN schemes are uniformly second-order accurate and may achieve genuinely third-order accuracy in the monotonic smooth regions of the solution. In this paper we will give two WEN schemes with the same stencils, but different accuracies.

· WEN1 scheme

Starting with the original ENN scheme (2.6) and (2.7), we weight not only first-order differences, but also second-order differences, appearing in the ENN scheme and give numerical fluxes of the WEN1 scheme

$$\left.\begin{aligned} h^+_{j+1/2} &= f^+_j + \frac{1}{2}(\omega^+_0 \Delta f^+_{j+1/2} + \omega^+_1 \Delta f^+_{j-1/2}) + \left(\frac{\omega^+_1}{2} - \frac{1}{6}\right) \cdot \\ &\quad (\theta^+_0 D^+_{j+1} + \theta^+_1 D^+_j + \theta^+_2 D^+_{j-1}) \\ h^-_{j+1/2} &= f^-_{j+1} - \frac{1}{2}(\omega^-_0 \Delta f^-_{j+3/2} + \omega^-_1 \Delta f^-_{j+1/2}) + \left(\frac{\omega^-_0}{2} - \frac{1}{6}\right) \cdot \\ &\quad (\theta^-_0 D^-_{j+2} + \theta^-_1 D^-_{j+1} + \theta^-_2 D^-_j) \end{aligned}\right\} \tag{2.8}$$

$$\omega_0^{\pm}=\frac{\alpha_0^{\pm}}{\alpha_0^{\pm}+\alpha_1^{\pm}} \qquad \omega_1^{\pm}=\frac{\alpha_1^{\pm}}{\alpha_0^{\pm}+\alpha_1^{\pm}} \qquad \alpha_0^{+}=\frac{1}{3(\varepsilon+(\mid \Delta f^{+}_{j+\frac{1}{2}} \mid)^p)}$$

$$\alpha_1^{+}=\frac{1}{6(\varepsilon+(\mid \Delta f^{+}_{j-\frac{1}{2}} \mid)^p)} \qquad \alpha_0^{-}=\frac{1}{6(\varepsilon+(\mid \Delta f^{-}_{j+\frac{3}{2}} \mid)^p)} \qquad \alpha_1^{-}=\frac{1}{3(\varepsilon+(\mid \Delta f^{-}_{j+\frac{1}{2}} \mid)^p)}$$

$$\theta_i^{\pm}=\frac{\beta_i^{\pm}}{\beta_1^{\pm}+\beta_2^{\pm}+\beta_3^{\pm}} \qquad i=1,2,3$$

$$\beta_0^{+}=\frac{1}{K_{j+1}(\varepsilon+(\mid D^{+}_{j+1} \mid)^p)} \qquad \beta_1^{+}=\frac{1}{K_j(\varepsilon+(\mid D^{+}_{j} \mid)^p)} \qquad \beta_2^{+}=\frac{1}{K_{j-1}(\varepsilon+(\mid D^{+}_{j-1} \mid)^p)}$$

$$K_j=(\varepsilon+(\mid \Delta f^{+}_{j+\frac{1}{2}} \mid)^p)(\varepsilon+(\mid \Delta f^{+}_{j-\frac{1}{2}} \mid)^p)$$

We can obtain β^- in the same way.

WEN2 scheme

In this case starting with 4th-order central-type numerical fluxes

$$h^{+}_{j+1/2}=\begin{cases} f_j^{+}+\dfrac{1}{2}\Delta f^{+}_{j+1/2}-\dfrac{1}{12}D_j^{+}-\dfrac{1}{12}D_{j+1}^{+} \\ \quad \text{if} \quad \mid \Delta f^{+}_{j+1/2} \mid \leq \mid \Delta f^{+}_{j-1/2} \mid \\ f_j^{+}+\dfrac{1}{2}\Delta f^{+}_{j-1/2}+\dfrac{1}{4}D_j^{+}+\dfrac{1}{12}D_{j-1}^{+} \\ \quad \text{if} \quad \mid \Delta f^{+}_{j+1/2} \mid > \mid \Delta f^{+}_{j-1/2} \mid \end{cases} \tag{2.9a}$$

$$h^{-}_{j+1/2}=\begin{cases} f_{j+1}^{-}-\dfrac{1}{2}\Delta f^{-}_{j+3/2}+\dfrac{1}{4}D_{j+1}^{-}+\dfrac{1}{12}D_{j+2}^{-} \\ \quad \text{if} \quad \mid \Delta f^{-}_{j+3/2} \mid \leq \mid \Delta f^{-}_{j+1/2} \mid \\ f_{j+1}^{-}-\dfrac{1}{2}\Delta f^{-}_{j+1/2}-\dfrac{1}{12}D_{j+1}^{-}-\dfrac{1}{12}D_{j}^{-} \\ \quad \text{if} \quad \mid \Delta f^{-}_{j+3/2} \mid > \mid \Delta f^{-}_{j+1/2} \mid \end{cases} \tag{2.9b}$$

we can construct another weight-type scheme of higher accuracy called the WEN2 scheme

$$\left.\begin{aligned} h^{+}_{j+1/2}&=f_j^{+}+\frac{1}{2}(\Omega_0^{+}\Delta f^{+}_{j+1/2}+\Omega_1^{+}\Delta f^{+}_{j-1/2})-\frac{\Omega_0^{+}}{6}(\Theta_0^{+}D^{+}_{j+1}+\Theta_1^{+}D_j^{+})+ \\ &\quad \frac{\Omega_1^{+}}{3}(\Phi_0^{+}D_j^{+}+\Phi_1^{+}D^{+}_{j-1}) \\ h^{-}_{j+1/2}&=f_{j+1}^{-}-\frac{1}{2}(\Omega_0^{-}\Delta f^{-}_{j+3/2}+\Omega_1^{-}\Delta f^{-}_{j+1/2})-\frac{\Omega_1^{-}}{6}(\Theta_0^{-}D^{-}_{j+1}+\Theta_1^{-}D_j^{-})+ \\ &\quad \frac{\Omega_0^{-}}{3}(\Phi_0^{-}D^{-}_{j+2}+\Phi_1^{-}D^{-}_{j+1}) \end{aligned}\right\} \tag{2.10}$$

where

$$\Omega_i^{\pm}=\frac{\alpha_i^{\pm}}{\alpha_0^{\pm}+\alpha_1^{\pm}},\qquad \Theta_i^{\pm}=\frac{\beta_i^{\pm}}{\beta_0^{\pm}+\beta_1^{\pm}},\qquad \Phi_i^{\pm}=\frac{\gamma_i^{\pm}}{\gamma_0^{\pm}+\gamma_1^{\pm}},\qquad i=0,1$$

$$\alpha_0^{+}=\frac{1}{\varepsilon+(\mid \Delta f_{j+1/2}^{+}\mid)^p} \qquad \alpha_1^{+}=\frac{1}{\varepsilon+(\mid \Delta f_{j-1/2}^{+}\mid)^p}$$

$$\beta_0^{+}=\frac{1}{(\varepsilon+(\mid D_{j+1}^{+}\mid)^p)} \qquad \beta_1^{+}=\frac{1}{(\varepsilon+(\mid D_{j}^{+}\mid)^p)}$$

$$\gamma_0^{+}=\frac{1}{4(\varepsilon+(\mid D_{j}^{+}\mid)^p)} \qquad \gamma_1^{+}=\frac{1}{12(\varepsilon+(\mid D_{j-1}^{+}\mid)^p)}$$

$$\alpha_0^{-}=\frac{1}{\varepsilon+(\mid \Delta f_{j+3/2}^{-}\mid)^p} \qquad \alpha_1^{-}=\frac{1}{\varepsilon+(\mid \Delta f_{j+1/2}^{-}\mid)^p}$$

$$\beta_0^{-}=\frac{1}{(\varepsilon+(\mid D_{j+1}^{-}\mid)^p)} \qquad \beta_1^{-}=\frac{1}{(\varepsilon+(\mid D_{j}^{-}\mid)^p)}$$

$$\gamma_0^{-}=\frac{1}{12(\varepsilon+(\mid D_{j+2}^{-}\mid)^p)} \qquad \gamma_1^{-}=\frac{1}{4(\varepsilon+(\mid D_{j+1}^{-}\mid)^p)}$$

In all WEN schemes, we take $\varepsilon=10^{-20}$ and $p=1.0$.

To examine the difference between the weighted and non-weighted schemes on accuracy, rate of convergence and robustness, we has performed in this section a comparative study of the different schemes for linear and nonlinear scalar equation.

Example 1. the linear initial problem

$$\left.\begin{array}{ll}\dfrac{\partial u}{\partial t}+\dfrac{\partial u}{\partial x}=0 & -1\leq x\leq 1\\ u(x,0)=\sin 2\pi x & -1\leq x\leq 1\end{array}\right\} \tag{2.11}$$

with periodic boundary conditions. Numerical solutions of different schemes are compared with the analytical solution at $t=2.0$ and for $\Delta t/\Delta x=0.5$.

Example 2. the linear initial problem

$$\left.\begin{array}{l}\dfrac{\partial u}{\partial t}+\dfrac{\partial u}{\partial x}=0 \qquad -1\leq x\leq 1\\ u(x+0.5,0)=\begin{cases}-x\sin(\dfrac{3\pi x^2}{2}) & -1<x<-\dfrac{1}{3}\\ \mid \sin(2\pi x)\mid & -\dfrac{1}{3}\leq x\leq\dfrac{1}{3}\\ 2x-1-\dfrac{1}{6}\sin(3\pi x) & \dfrac{1}{3}<x<1\end{cases}\end{array}\right\} \tag{2.12}$$

with periodic boundary conditions, $t=2$ and $\Delta t/\Delta x=0.5$.

Example 3. the nonlinear Burgers equation

$$\left.\begin{array}{l}\dfrac{\partial u}{\partial t}+\dfrac{\partial(\frac{u^2}{2})}{\partial x}=\varepsilon\dfrac{\partial^2 u}{\partial x^2}\\ u(x,0)=f(x)\\ u(-1,t)=1 \qquad u(1,t)=-1\end{array}\right\} \tag{2.13}$$

In computation $\varepsilon = 0.001$ and $\Delta t/\Delta x = 0.5$. The steady solutions as $t \to \infty$, are found for different schemes.

From Figs.1~4 we can see that the WND scheme enhances significantly the accuracy near the extrema. Figure 5 and Fig.6 show the WND scheme keeps the non-oscillatory property and improves the resolution of shock.

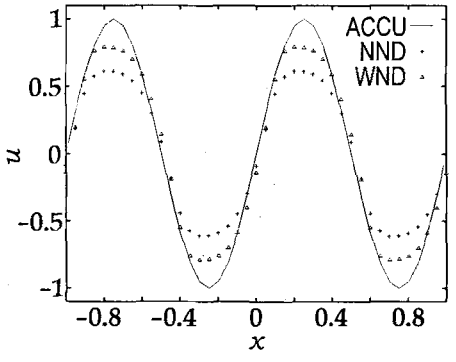

Fig.1 $N = 40$

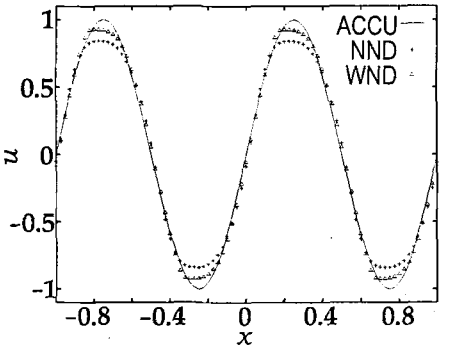

Fig.2 $N = 80$

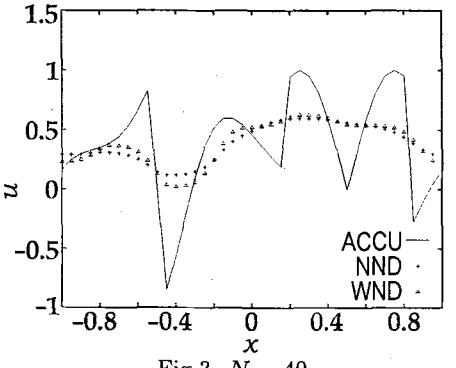

Fig.3 $N = 40$

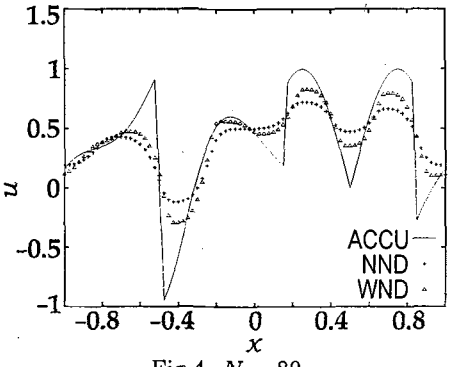

Fig.4 $N = 80$

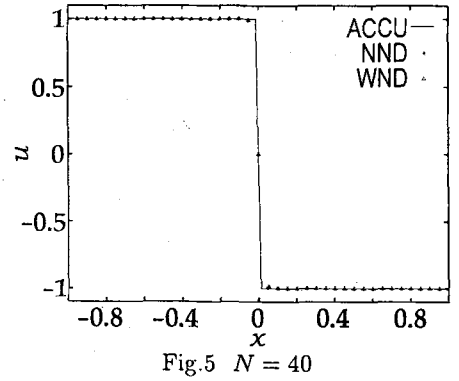

Fig.5 $N = 40$

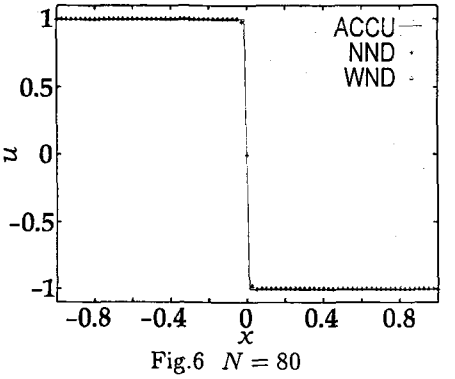

Fig.6 $N = 80$

Figures 7~12 display that the WEN1 scheme is of the same accuracy as the ENN scheme in any regions, but we will see later that the WEN1 scheme has higher accuracy in vortex regions and quite fast rate of convergence to the steady solution for the two-dimensional shock/boundary layer interaction problem. From Fig.9 and Fig.10 we can see

also that the WEN2 scheme has higher accuracy near the extrema than that of the ENN and WEN1 schemes. Figure 11 and Fig.12 show the WEN1 and WEN2 schemes can keep the non-oscillatory property.

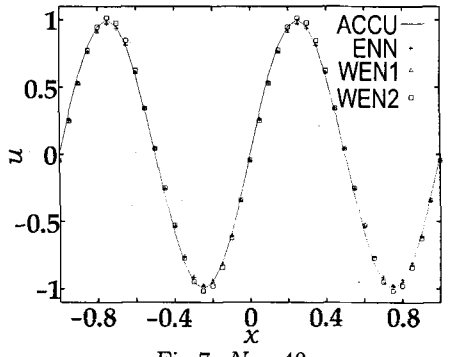

Fig.7 $N = 40$

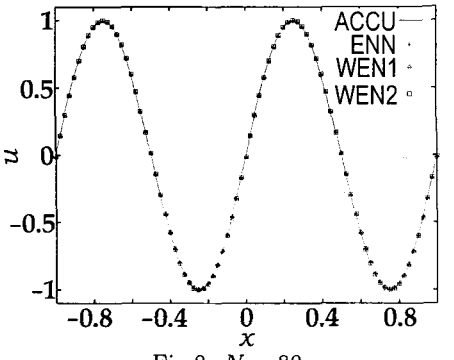

Fig.8 $N = 80$

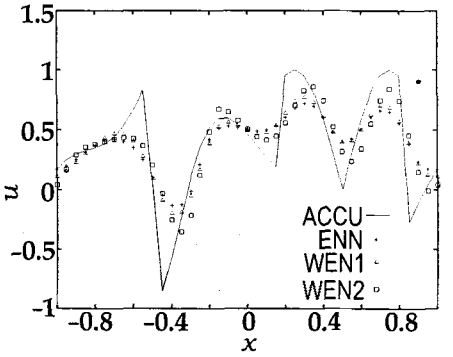

Fig.9 $N = 40$

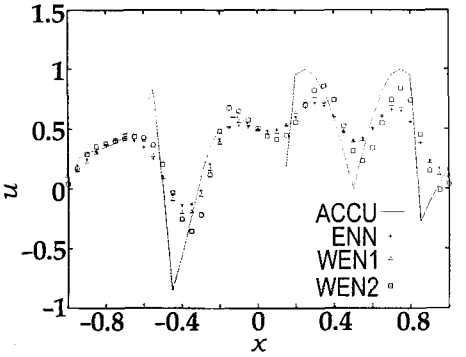

Fig.10 $N = 80$

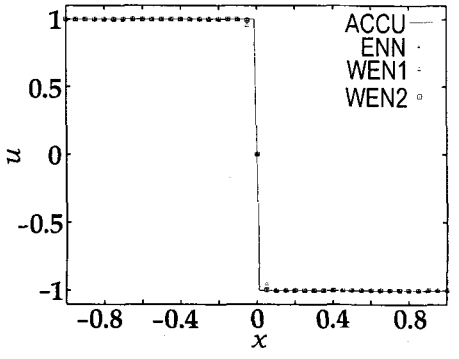

Fig.11 $N = 40$

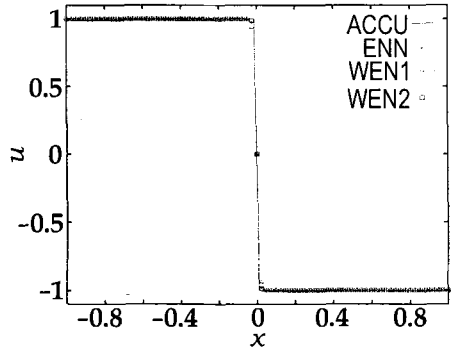

Fig.12 $N = 80$

3 DIFFERENCE SCHEMES FOR HYPERBOLIC SYSTEMS OF CONSERVATION LAWS

Consider the following conservative hyperbolic system of equations

$$\frac{\partial \boldsymbol{U}}{\partial t} + \frac{\partial \boldsymbol{F}(\boldsymbol{U})}{\partial x} = 0 \tag{3.1}$$

where $\boldsymbol{U} = (u_1, u_2, ..., u_m)^{\mathrm{T}}$ is a vector of conserved variables and $\boldsymbol{F}(\boldsymbol{U}) = (f^1(\boldsymbol{U}), f^2(\boldsymbol{U}),$

$\cdots, f^m(\boldsymbol{U}))^{\mathrm{T}}$ is a flux vector and $\boldsymbol{A} = \dfrac{\partial \boldsymbol{F}(\boldsymbol{U})}{\partial \boldsymbol{U}}$, let $\boldsymbol{\Lambda} = \mathrm{diag}(\lambda^1, \lambda^2, \cdots, \lambda^m)$ be a diagonal matrix consisting of the eigenvalues of the matrix $\boldsymbol{A}$ and $\boldsymbol{A} = \boldsymbol{R}\boldsymbol{\Lambda}\boldsymbol{R}^{-1}$. $\boldsymbol{R}$ is a matrix, the columns of which are the right eigenvectors of $\boldsymbol{A}$. In the following we will give only the WND scheme in two versions.

3.1 WND Scheme in Version of the Flux Vector Splitting

In this paper the Steger-Warming flux vector splitting is used, i.e. let $\lambda^{\pm l} = \dfrac{1}{2}(\lambda^{\pm l} \pm |\lambda^{\pm l}|)$and $\boldsymbol{\Lambda}^{\pm} = \mathrm{diag}(\lambda^{\pm l})(l = 1, 2, \cdots, m)$. We have $\boldsymbol{A}^{\pm} = \boldsymbol{R}\boldsymbol{\Lambda}^{\pm}\boldsymbol{R}^{-1}$, $\boldsymbol{F}^{\pm} = \boldsymbol{A}^{\pm}\boldsymbol{U}$, $\Delta \boldsymbol{F}^{\pm}_{j+1/2} = \boldsymbol{F}^{\pm}_{j+1} - \boldsymbol{F}^{\pm}_{j}$. In this case, the semi-discrete WND scheme takes the form

$$\left(\frac{\mathrm{d}\boldsymbol{U}}{\mathrm{d}t}\right)^{n+1}_{j} + \frac{\boldsymbol{h}_{j+1/2} - \boldsymbol{h}_{j-1/2}}{\Delta x} = 0 \tag{3.2}$$

$$\boldsymbol{h}_{j+1/2} = \boldsymbol{F}^{+}_{j} + \boldsymbol{F}^{-}_{j+1} + \frac{1}{2}(\Omega^{+}_{0}\Delta \boldsymbol{F}^{+}_{j+1/2} + \Omega^{+}_{1}\Delta \boldsymbol{F}^{+}_{j-1/2}) - \frac{1}{2}(\Omega^{-}_{0}\Delta \boldsymbol{F}^{-}_{j+3/2} + \Omega^{-}_{1}\Delta \boldsymbol{F}^{-}_{j+1/2}) \tag{3.3}$$

where

$$\Omega^{\pm}_{i} = \mathrm{diag}(\omega^{\pm 1}_{i}, \omega^{\pm 2}_{i}, \cdots, \omega^{\pm m}_{i}) \qquad \Omega^{\pm}_{0} + \Omega^{\pm}_{1} = \mathrm{diag}(1, 1, ..., 1)$$

$$\omega^{\pm k}_{i} = \frac{\alpha^{\pm k}_{i}}{\alpha^{\pm k}_{0} + \alpha^{\pm k}_{1}} \qquad \alpha^{+k}_{0} = \frac{1}{\varepsilon + \left|\Delta f^{+k}_{j+1/2}\right|}$$

$$\alpha^{+k}_{1} = \frac{1}{\varepsilon + \left|\Delta f^{+k}_{j-1/2}\right|} \qquad \alpha^{-k}_{0} = \frac{1}{\varepsilon + \left|\Delta f^{-k}_{j+3/2}\right|}$$

$$\alpha^{-k}_{1} = \frac{1}{\varepsilon + \left|\Delta f^{-k}_{j+1/2}\right|} \qquad (i = 0, 1;\ k = 1, 2, ..., m;\ \varepsilon = 10^{-10})$$

3.2 WND Scheme in Version of the Flux-Difference Splitting

$$\begin{aligned}\boldsymbol{H}_{j+1/2} = {} & \frac{1}{2}\left(\boldsymbol{F}_{j+1} + \boldsymbol{F}_{j} - \boldsymbol{R}_{j+1/2}\left|\boldsymbol{\Lambda}_{j+1/2}\right|\boldsymbol{R}^{-1}_{j+1/2}\Delta \boldsymbol{U}_{j+1/2}\right) + \\ & \frac{1}{2}\boldsymbol{R}_{j+1/2}\left(\Omega^{+}_{1}\boldsymbol{\Lambda}^{+}_{j+1/2}\boldsymbol{R}^{-1}_{j+1/2}\Delta \boldsymbol{U}_{j+1/2} + \Omega^{+}_{2}\boldsymbol{\Lambda}^{+}_{j-1/2}\boldsymbol{R}^{-1}_{j-1/2}\Delta \boldsymbol{U}_{j-1/2}\right) - \\ & \frac{1}{2}\boldsymbol{R}_{j+1/2}\left(\Omega^{-}_{1}\boldsymbol{\Lambda}^{-}_{j+1/2}\boldsymbol{R}^{-1}_{j+1/2}\Delta \boldsymbol{U}_{j+1/2} + \Omega^{-}_{2}\boldsymbol{\Lambda}^{-}_{j+3/2}\boldsymbol{R}^{-1}_{j+3/2}\Delta \boldsymbol{U}_{j+3/2}\right)\end{aligned} \tag{3.4}$$

where

$$\Omega^{\pm}_{i} = \mathrm{diag}(\omega^{\pm 1}_{i}, \omega^{\pm 2}_{i}, \cdots, \omega^{\pm m}_{i})$$

$$\boldsymbol{\Lambda}^{\pm}_{j+1/2} = \mathrm{diag}\left(\frac{\lambda^{1}_{j+\frac{1}{2}} \pm \left|\lambda^{1}_{j+\frac{1}{2}}\right|}{2}, \cdots, \frac{\lambda^{m}_{j+\frac{1}{2}} \pm \left|\lambda^{m}_{j+\frac{1}{2}}\right|}{2}\right)$$

$$\omega_1^{k\pm}=\frac{\beta_1^{k\pm}}{\beta_1^{k\pm}+\beta_2^{k\pm}} \qquad \omega_2^{k\pm}=\frac{\beta_2^{k\pm}}{\beta_1^{k\pm}+\beta_2^{k\pm}}$$

$$\beta_1^{k+}=\frac{1}{\varepsilon+\left|\frac{\lambda_{j+1/2}^k+\left|\lambda_{j+1/2}^k\right|}{2}\alpha_{j+1/2}^k\right|} \qquad \beta_2^{k+}=\frac{1}{\varepsilon+\left|\frac{\lambda_{j-1/2}^k+\left|\lambda_{j-1/2}^k\right|}{2}\alpha_{j-1/2}^k\right|}$$

$$\beta_1^{k-}=\frac{1}{\varepsilon+\left|\frac{\lambda_{j+1/2}^k-\left|\lambda_{j+1/2}^k\right|}{2}\alpha_{j+1/2}^k\right|} \qquad \beta_2^{k-}=\frac{1}{\varepsilon+\left|\frac{\lambda_{j+3/2}^k-\left|\lambda_{j+3/2}^k\right|}{2}\alpha_{j+3/2}^k\right|}$$

$(i=0,1;\ k=1,2,...,m)$

$$\boldsymbol{\alpha}_{j+1/2}=\boldsymbol{R}_{j+1/2}^{-1}\Delta\boldsymbol{U}_{j+1/2}=(\alpha_{j+1/2}^1,\ \alpha_{j+1/2}^2,\cdots,\alpha_{j+1/2}^m)^{\mathrm{T}}$$

In our computation the Roe averages are used for $\boldsymbol{R}_{j+1/2}, \boldsymbol{R}_{j+1/2}^{-1}, \boldsymbol{\Lambda}_{j+1/2}$.

Numerical experiments showed that the scheme (3.2), (3.4) is more accurate than the scheme(3.2), (3.3). In this paper the scheme (3.2), (3.4) is adopted, and in fact it is a weighted Roe's scheme.

4 APPLICATION TO PROBLEM OF VISCOUS FLOW

In this section the advantages of the WND and WEN schemes will be demonstrated by solving the Navier-Stokes equations for the flat plate shock/boundary layer interaction problem.

As is well known, the flat plate shock/boundary-layer interaction problem has become a benchmark of testing new numerical methods for viscous flow[5,6]. In this paper, computational parameters are $M_\infty=2.0$, $Re_\infty=2.96\times10^5$, $T_\infty=293\,\mathrm{K}$, $\gamma=1.4$, $Pr=0.72$.

Following [6], the computational domain is chosen to be $0\le x\le0.32$, $0\le y\le0.1215$, the reference length $\overline{L}=0.16$, the impinging shock angle is $\theta=32.585°$.

The computation was carried out with 33×33 and 65×65 grid points. A criterion of convergence to a steady solution is defined as follows

$$E=\frac{1}{n_x\cdot n_y}\sum_{i=1}^{n_x}\sum_{j=1}^{n_y}\left\{\left|\frac{\Delta\rho}{\Delta t}\right|+\left|\frac{\Delta\rho u}{\Delta t}\right|+\left|\frac{\Delta\rho v}{\Delta t}\right|+\left|\frac{\Delta E}{\Delta t}\right|\right\}_{ij}\le0.5\times10^{-3} \tag{4.7}$$

For solving the two-dimensional time-dependent Navier-Stokes equations, an explicit-implicit scheme is adopted, i.e. the scheme is explicit in the flow direction and implicit in the direction normal to the flat plate. Numerical test was performed with the NS and PNS equations, respectively. We found that numerical results show no significant difference between both classes of equations for the given freestream conditions in this paper.

In Table 1 and Table 2 comparisons of the convergence rate of different schemes are given with 33×33 and 65×65 grids. In Table 1 the WND scheme is about twice as fast as

Table 1 Comparison of rate of convergence to steady state for shock boundary-layer interactions (33×33)

Scheme	Time Step Number	$(C_f)_{\min}$	Convergence error(E)	CPU time(second)
NND	2500	-0.2066×10^{-3}	0.9235×10^{-3}	1276
WND	1016	-0.4185×10^{-3}	0.4984×10^{-3}	542

Note: The convergence error requires $E\le0.5\times10^{-3}$.

Table 2 Comparison of rate of convergence to steady state for shock boundary-layer interactions (65 × 65)

Scheme	Time Step Number	$(C_f)_{\min}$	Convergence error(E)
NND	15 000	-0.4387×10^{-3}	0.6228×10^{-3}
WND	4 274	-0.5662×10^{-3}	0.4988×10^{-3}

the NND scheme on the coarsest grid 33 × 33 and in Table 4 it is about four times as fast as the NND scheme on the finer grid 65 × 65.The NND scheme is getting slower and slower than the WND, when the grid points are increased.

Table 3 and Table 4 are comparisons of the convergence rates of the ENN, WEN1 and WEN2 schemes on the grid points 33 × 33 and 65 × 65 for the same problem. Among them, the WEN1 scheme is a robust and faster convergent than the ENN and the WEN1 scheme requires only 1341 iterations to achieve the steady solution within an allowable error.

Table 3 Comparison of rate of convergence to steady state for shock boundary-layer interactions (33 × 33)

Scheme	Time Step Number	$(C_f)_{\min}$	Convergence error(E)
ENN	4000	-0.3516×10^{-3}	0.8985×10^{-2}
WEN1	1341	-0.4510×10^{-3}	0.4997×10^{-3}
WEN2	4000	-0.6193×10^{-3}	0.1401×10^{-2}

Table 4 Comparison of rate of convergence to steady state for shock boundary-layer interactions (65 × 65)

Scheme	Time Step Number	$(C_f)_{\min}$	Convergence error(E)
ENN	15 000	-0.5245×10^{-3}	0.1920×10^{-1}
WEN1	4 899	-0.5894×10^{-3}	0.4999×10^{-3}
WEN2	15 000	-0.5924×10^{-3}	0.2213×10^{-2}

Although the WEN2 scheme is also slower than the WEN1 scheme, it has very high accuracy in the vortex region. This fact may be validated by numerical results in [5].

Figures 13~16 show distributions of coefficient of skin friction and wall pressure obtained by the NND and WND schemes with 33 × 33 and 65 × 65 grids, respectively. Clearly, the coefficients of skin friction in the vortex region obtained by the WND scheme is more accurate and close the NND and WND to that given by the central scheme in [5]. Figures 17~18 are pressure contours obtained by schemes with 65 × 65 grids.

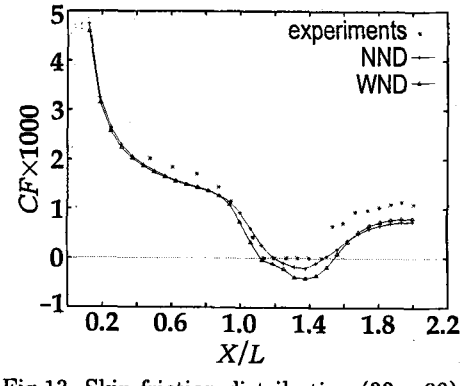

Fig.13 Skin friction distribution (33 × 33)

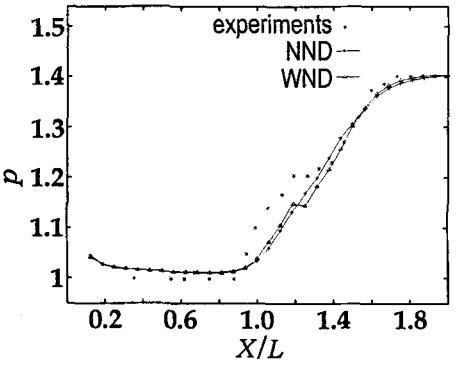

Fig.14 Wall pressure distribution (33 × 33)

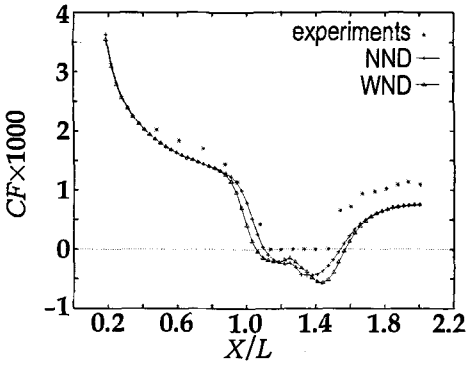

Fig.15 Skin friction distribution (65 × 65)

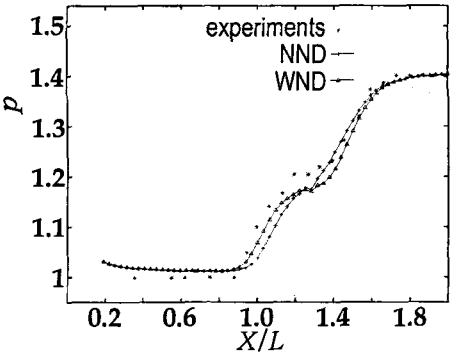

Fig.16 Wall pressure distribution (65 × 65)

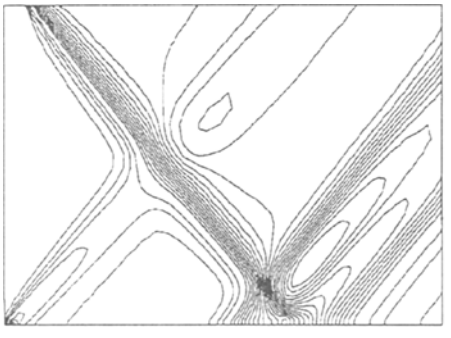

Fig.17 NND

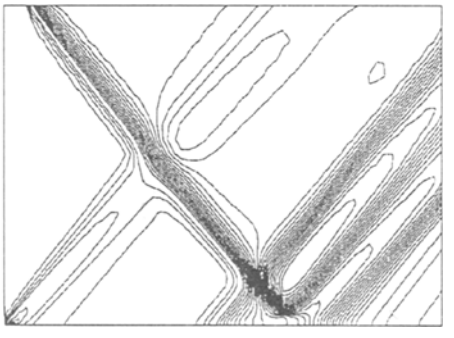

Fig.18 WND

Figures 19~22 are the same distributions of coefficient of skin friction and pressure obtained by the ENN, WEN1 and WEN2 schemes with 33×33 and 65×65 grids, respectively. An obvious difference between the ENN and WEN schemes in the separated vortex can be seen on the coarsest grid (33 × 33). Figures 23~24 display pressure contours obtained by the ENN and WEN1 schemes, respectively. We can see that the WND and WEN schemes have higher resolution of the shocks and vortex than that of the NND and ENN schemes.

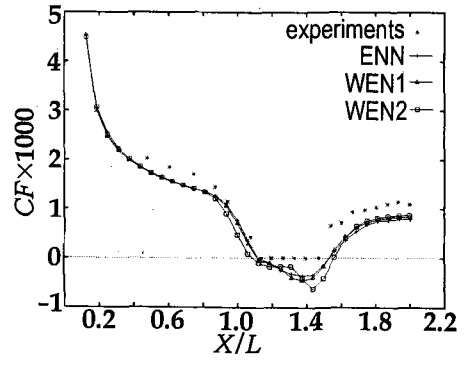

Fig:19 Skin friction distribution (33 × 33)

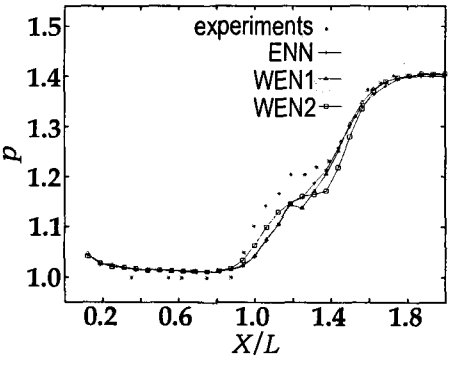

Fig.20 Wall pressure distribution (33 × 33)

Acknowledgement We would like to thank Professor Chi-wang Shu for helpful discussions and suggestions.

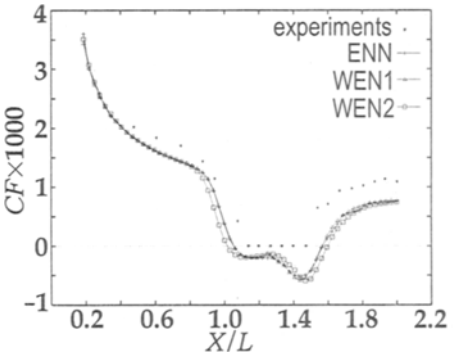

Fig.21 Skin friction distribution (65 × 65)

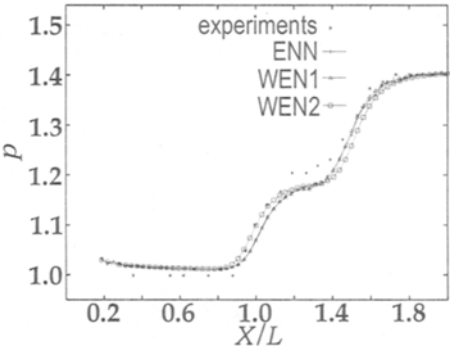

Fig.22 Wall pressure distribution (65 × 65)

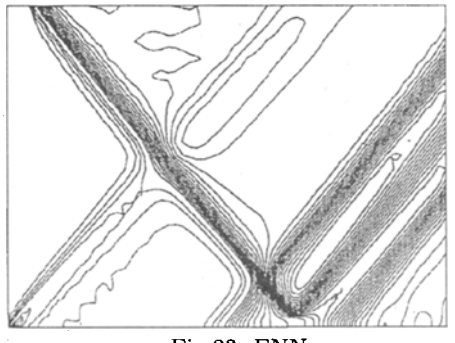

Fig.23 ENN

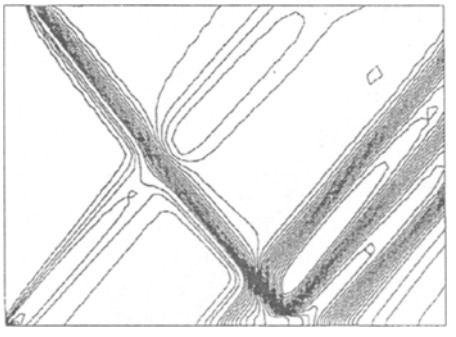

Fig.24 WEN1

REFERENCES

1 Liu XD, Osher S, Chan T. Weighted essentially non-oscillatory schemes. *J Comput Phys*, 1994, 115: 200~212

2 Jiang GS, Shu CW. Efficient implementation of weighted ENO schemes. *J Comput Phys*, 1996, 125: 202~228

3 Zhang Hanxin. Non-oscillatory and non-free-parameter dissipation difference scheme. *Acta Aerodynamica Sinica*, 1988, 6(2): 143~165 (in Chinese)

4 Zhang Hanxin, He Guohong, Zhang Lei. Some important problems for high-order accurate difference schemes for solving gas dynamic equations. *Acta Aerodynamica Sinica*, 1993, 11(4): 347~356 (in Chinese)

5 MacCormark RW. Numerical solution of the interaction of a shock wave with a laminar boundary layer. In: Lecture Notes in Physics. Ed. Maurice Holt, Berlin: Springer-Verlag, 1971, 8: 153~163

6 Wang Z, Richards BE. Higher resolution schemes for steady flow computation. *J Comput Phys*, 1991, 97: 53~72